Thermal, magnetic, and transport properties of single-crystal $Sr_{1-x}Ca_xRuO_3$ ($0 \leqslant x \leqslant 1.0$)

G. Cao, S. McCall, M. Shepard, and J. E. Crow
National High Magnetic Field Laboratory, Florida State University, Tallahassee, Florida 32310

R. P. Guertin*
Physics Department, Tufts University, Medford, Massachusetts 02155

(Received 24 January 1997)

$SrRuO_3$ is a highly correlated, narrow d-band metal which undergoes a ferromagnetic transition at $T_c = 165$ K. $CaRuO_3$, which is also a highly correlated metal, has the same crystal structure, comparable electrical resistivity and similar effective Ru moment, but it remains paramagnetic at least down to 1 K. High- and low-field magnetization and susceptibility, thermoremanent magnetization, low-temperature heat capacity, electrical resistivity, and Hall effect measurements are presented on as-grown, untwinned, orthorhombic single-crystal samples of $Sr_{1-x}Ca_xRuO_3$ for the entire concentration range $0 \leqslant x \leqslant 1.0$. T_c is depressed uniformly with increasing x, all the way to $x = 1.0$, with possible spin-glass-type ordering for x close to 1.0. The critical Sr doping of paramagnetic $CaRuO_3$ required to cause magnetic correlations among the Ru moments is $\cong 1$ at.%. Magnetization to 7 T shows strong hysteresis for mixed ($x > 0$) crystals only, with evidence for a rotation of the easy magnetic axis out of the ab plane. Low-temperature magnetization in dc fields to 30 T for $x = 0$ shows a lack of saturation to the full $S = 1$ moment, $2\mu_B$/Ru atom, underscoring the itinerant character of the ferromagnetism. Similar data for $x = 1.0$ show it to be a highly exchange enhanced paramagnet, a borderline antiferromagnet or ferromagnet. This is consistent with previous Ru-O in-plane and out-of-plane doping studies. Low-temperature heat capacity ($1 < T < 20$ K) shows that the mass enhancement ($\gamma = 29$ mJ/mol K^2 and $m^* \approx 3$ for $x = 0$) and the Debye temperature ($\Theta_D = 390$ K for $x = 0$) are nonmonotonically varying with increasing x. The large electrical resistivity suggests these materials are ''bad'' metals, with a mean free path at room temperature ≈ 10 A for $x = 0$. The Hall effect shows a sign reversal for $x = 0$ and $x = 1.0$, but not for mixed crystals. The data are compared where it is appropriate to data derived from comparable experiments from polycrystalline samples and from epitaxially grown thin films. The results support the highly electron-correlated nature of ordered magnetism in Ru-based oxides and the results should help to advance our understanding of the transport, magnetic, and thermodynamic properties of bad metals. [S0163-1829(97)03025-7]

INTRODUCTION

Although it has been 40 years since the rather remarkable and unexpected discovery of ferromagnetism in the nearly cubic perovskite $SrRuO_3$, a thorough understanding of the electronic properties of that metallic transition-metal oxide has remained elusive.[1] The Curie temperature $T_C = 165$ K is rather large, and the ordered magnetic moment within the ferromagnetic phase is variously reported between $0.8\mu_B$/Ru and $1.6\mu_B$/Ru. The Ru moment is in the ''low-spin'' ($S = 1$) state: The octahedral crystalline electric field of O atoms splits the fivefold degeneracy of the Ru $4d^4$ configuration into a triplet (t_{2g}) ground state, two-thirds occupied, and a doublet (e_g) excited state, unoccupied. Modification of the free ion moment through electron correlation effects causes the observed nonintegral saturation moment.[2] Like other transition-metal oxides, the magnetic, transport, and low-temperature thermodynamic properties of $SrRuO_3$ and related ruthenates are influenced heavily by the covalent coupling of the Ru d shell to the O $2p$ electrons. This coupling should be stronger for extended $4d$ transition-metal oxides like Ru than for the $3d$'s, which have to date been far more extensively studied.

A narrow d-band model reflective of strong electron-electron correlations is useful in understanding the physical properties of many transition-metal oxides.[3] The Mott-Hubbard model for characterizing metals and insulators involves the ratio W/U, where W is the d-band width and U the intra-atomic Coulomb repulsion. For $W/U \gg 1$, metallic behavior is expected, for $W/U \ll 1$, insulating. That $SrRuO_3$ shows a metallic temperature dependence of the electrical resistivity ($d\rho/dT > 0$) is consistent with this: The $4d$ shell of Ru has a greater extent than for comparable $3d$ elements, thus weakening U in comparison with $3d$ transition-metal oxides. In addition, the greater extent of the Ru $4d$ shell should also promote Ru-Ru coupling—coupling that is mediated by the intervening O atom. $SrRuO_3$ has been characterized as a ''bad'' metal because the resistivity continues to increase above room temperature, even though the calculated Boltzmann mean free path $l \cong 10$ Å becomes less than a lattice constant[4] or, stated alternatively, $k_F l \leqslant 1$. As the temperature is lowered in our single crystals, ρ decreases, $\rho_{300}/\rho_{10} \approx 50$, before saturating for $T < 10$ K. In $SrRuO_3$ the covalency of the Ru($4d$)-O($2p$) hybridization is underscored by recent polarized neutron-scattering results showing approximately 10% of the ordered magnetic moment associated with the O sites.[5]

The electronic structure of transition-metal oxides underlies the enormous range of their physical properties: from insulating to superconducting, from diamagnetic to ferro-

magnetic. The vast preponderance of research on transition-metal oxides has been on the $3d$ members, not the least of which is due to high-temperature superconductivity in the cuprates and colossal magnetoresistance in the doped manganese oxides. These studies have in turn spurred research in $4d$ and $5d$ metallic oxides, and in the ruthenates, in particular, sparked by the discovery of superconductivity ($T_c = 0.93$ K) in single-crystal Sr_2RuO_4 (Ref. 6) and the speculation of superconductivity at much higher temperatures. To date, only the ruthenates among the $4d$ oxides show long-range magnetic order. Within the last two years, several reports were published on measurements in $SrRuO_3$ and derivative transition-metal oxides. These include the following: Precise measurements on thin-film $SrRuO_3$ showing non-mean-field behavior of the critical exponents[7] of magnetization and electrical resistivity, a strong depression of T_C with pressure,[8] heat capacity and transport measurements compared to band structure calculations which reinforce the nonlocal character of the Ru moment,[4] a sign reversal of the Hall constant from electronlike to holelike as the temperature is increased,[4,9] temperature-dependent x-ray measurements showing a near-zero thermal expansion for $T < T_C$,[10] and based on high-temperature perturbed angular correlation measurements, a small structural transition to less than cubic symmetry below 800 K.[11]

It has been known for many years that $CaRuO_3$ the isomorphic transition-metal oxide to $SrRuO_3$, does not order magnetically, down to at least 1 K,[12] though the magnetic susceptibility is rather large and temperature dependent: $\chi = 12\times10^{-3}$ emu/mol at $T=4$ K and 2×10^{-3} at 300 K with an effective paramagnetic moment $\mu_{\rm eff}=2.2\mu_B$/Ru from a modified Curie-Weiss fit.[13] $CaRuO_3$ and $SrRuO_3$ are similar in several ways: Both have a similar orthorhombically distorted perovskite structure—$CaRuO_3$ is more distorted, as expected, because the Ca ionic radius (0.99 Å) is even less ideal for perovskite formation than Sr (1.18 Å), though they have similar (to 2%) lattice constants. Their metallic resistivities are comparable ($CaRuO_3$ with $\rho = 220\ \mu\Omega$ cm and $SrRuO_3$ with $\rho = 195\ \mu\Omega$ cm at room temperature). It is very likely they have similar electronic band structures in the paramagnetic regime.

Goodenough[2] suggests that the $CaRuO_3$ d-band width is narrower than for $SrRuO_3$, too narrow for magnetic ordering, but not so narrow as to cause $CaRuO_3$ to be nonmetallic ($W/U \ll 1$). This latter property suggests that $CaRuO_3$ is close to being an insulator and very near the magnetic-to-nonmagnetic transition boundary. Previous experiments on doping in single-crystal $CaRuO_3$ demonstrate this: Sn substitution for Ru in excess of 15 at. % induces a metal-to-insulator transition,[14] as does Rh in excess of 7%.[15] Furthermore, 5 at. % Na substitution for Ca induces antiferromagnetic or spin glass ordering at $T=55$ K,[13] and the conductivity decreases, though no transition to an insulating state is found—as it is for $SrRuO_3$ for slightly higher Na doping.[13]

The purpose of this paper is to present the results of a comprehensive study of the thermodynamic and transport properties on mixed single-crystal $SrRuO_3$ and $CaRuO_3$, namely, $Sr_{1-x}Ca_xRuO_3$, for $0 \leqslant x \leqslant 1.0$. We have also extended previous magnetization studies to higher dc fields (30 T) on the end member samples $x=0$ and $x=1.0$. Prior studies of $Sr_{1-x}Ca_xRuO_3$ have relied primarily on polycrystalline materials generated by ceramic techniques or on thin films of $SrRuO_3$. Examination of the literature shows a variability of critical properties among polycrystalline materials, and though the quality of the thin films is high, they appear slightly strained because the T_C reported for single-crystal $SrRuO_3$ is consistently lower than $T_C=165$ K measured in our high-quality single crystals. It is well known that T_C of $SrRuO_3$ decreases rather rapidly with pressure.[8]

The data presented here on single-crystal samples of $Sr_{1-x}Ca_xRuO_3$ show a smooth evolution with increasing x from long-range ferromagnetism ($x=0$) to a highly enhanced paramagnetic response ($x=1.0$). We find evidence for short-range magnetic ordering, possible spin glass behavior, for samples with only very little Sr content ($x\approx0.95$). Taking advantage of single-crystal materials, we present the magnetic anisotropy and associated magnetic hysteresis as a function of x. This is quite small for $x=0$, but grows as T_C is depressed to 0 K. Very-high-field magnetization measurements (to 30-T dc fields) show a field dependence even to the highest fields, underscoring the itinerant nature of the magnetism in this system. The mass enhancement and Debye temperature from heat capacity show two maxima as a function of x with a reproducible minimum for $x=0.5$. Finally, the temperature dependence of the Hall effect is presented over the series, showing a sign reversal for the end members, as seen recently,[9] but the sign reversal is not observed in the mixed systems.

SAMPLE PREPARATION AND EXPERIMENTAL DETAILS

The single-crystal samples were grown from a self-flux in Pt crucibles heated to 1500 °C using off-stoichiometric quantities of RuO_2, $SrCO_3$ (and/or $CaCO_3$ for mixed or pure samples), and $SrCl_2$ (or $CaCl_2$), a self-flux. The samples were soaked at 1500 °C for 25 h, cooled slowly at 2 °C/h to 1350 °C, and then rapidly quenched to room temperature to avoid possible twinning. The Sr:Ru starting ratio is essential to achieve the desired stoichiometry. Energy-dispersive x-ray analysis (EDAX) scanning electron microscopy (SEM) and x-ray diffraction were used to determine composition and phase integrity.

All samples showed the ABO_3 composition and $GdFeO_3$ orthorhombic structure with no secondary phases detected. The morphology of the samples was consistent: They tend to form as 1–2 mg rectangular parallelepipeds, with the short dimension along the c direction [001]. All measurements were carried out on ''as-grown'' single crystals.

The surfaces of several of the crystals were examined in polarized light with a differential interference contrast microscope. There was no evidence of twinning in the ab plane of the crystals down to a scale of $\approx1\ \mu$m. As with thin-film specimens,[16] the single crystals are fully stable when exposed for long periods to the atmosphere. This property is particularly important, as thin-film $SrRuO_3$ and derivative materials have been cited as potentially useful substrate materials for device applications involving other oxide materials such as high-temperature superconducting cuprates.

Figure 1 shows the concentration dependence of the room-temperature lattice parameters for five representative

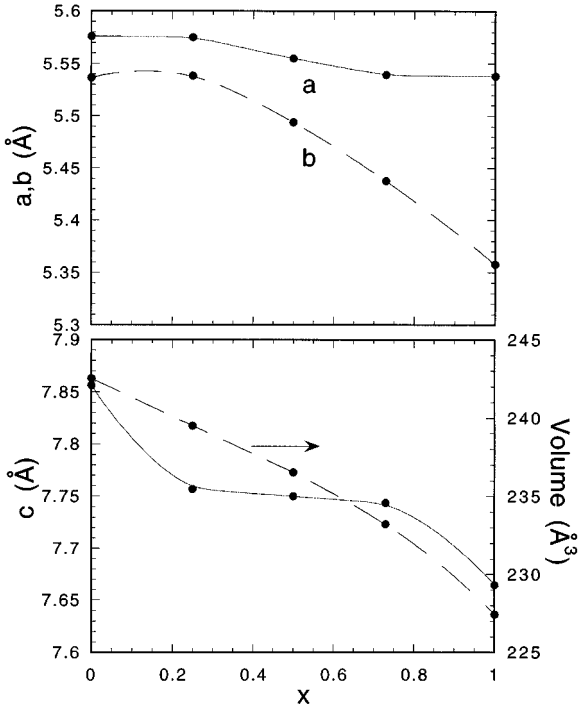

FIG. 1. Room-temperature lattice constants vs x for $Sr_{1-x}Ca_xRuO_3$.

$Sr_{1-x}Ca_xRuO_3$ samples. The a-b splitting grows with increasing x. This reflects the smaller ionic radius of Ca and the slightly more distorted, less ideal perovskite, structure of $CaRuO_3$ compared to $SrRuO_3$. These lattice constants are identical with those reported for thin films.[16] It is somewhat surprising, therefore, that the reported Curie temperature for the 1000-Å thin-film $SrRuO_3$ sample is only 150 K, compared to $T_C = 165$ K in our single-crystal sample. If the thin films are strained, which could explain the lower T_C, the strain is not enough to alter the reduce lattice constants as measured with x rays. However, $SrRuO_3$ thin films often show a somewhat larger room-temperature electrical resistivity compared to the ab-plane resistivity measured on our single crystals ($\rho \approx 300\ \mu\Omega$ cm vs $200\ \mu\Omega$ cm; see Refs. 7, 16, and 17 and this work), indicating possible effects of strain. We also note that slight changes in the Sr:Ru ratio can strongly alter T_C.

Magnetization studies were performed on a quantum design superconducting quantum interference device (SQUID) MPMS system ($2 \leqslant T \leqslant 400$ K, $0 \leqslant H \leqslant 7$ T), and for higher fields a vibrating sample magnetometer, installed on a 30-T resistive magnet of the National High Field Magnet Laboratory, was used. Resistivity studies were performed with the standard four-lead technique and in a 12-T superconducting solenoid, and the Hall effect was measured with a six-lead van der Pauw technique. Heat capacity was carried out for $1 < T < 20$ K using a low-mass heat capacity system with a sensitivity of about 1 μJ/K for a 1-mg, sample at 10 K.

EXPERIMENTAL RESULTS: MAGNETIC PROPERTIES

In Fig. 2 we show the magnetic susceptibility $\chi(T)$ measured in a field $H = 0.1$ T for several $Sr_{1-x}Ca_xRuO_3$ samples in their respective paramagnetic ($T > T_C$) regimes. Note the

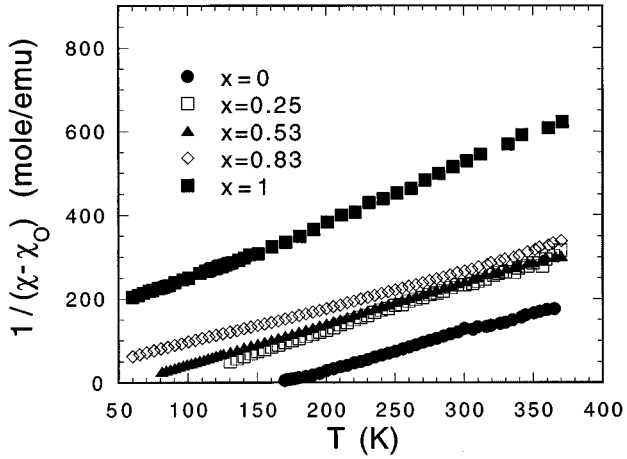

FIG. 2. Curie-Weiss plot of the magnetic susceptibility ($H = 0.1$ T) of $Sr_{1-x}Ca_xRuO_3$ plotted to fit the modified Curie-Weiss law $\chi(T) = \chi_0 + C/(T - \Theta)$.

data of Fig. 2 cover the temperature interval $50 < T < 400$ K. All data generally showed agreement with the modified Curie-Weiss law: $\chi(T) = \chi_0 + C/(T - \Theta)$, where χ_0 represents a term reflecting the Pauli susceptibility χ_p, Landau diamagnetism, and core diamagnetism, C is the Curie constant, and Θ is the Curie-Weiss (CW) temperature. Fits to the CW law were less good near T_C as expected because of short-range order and fluctuation effects. The parameters of the fits to these data, taken over the temperature interval from about 30 K above T_C to 380 K, are shown in Table I.

In these highly correlated, narrow d-band materials, we expect χ_p to dominate, and so we take χ_0 to be proportional to χ_p and, hence, the density of states at the Fermi surface. This allows us to compare these values of the density of states with those obtained from the low-temperature electronic contribution to the heat capacity. For $0 < x < 0.5$ the Curie constants were close to 1.00 emu K/mol, corresponding to the $S = 1$ effective paramagnetic moment, $2.8\mu_B$/Ru atom, and show a modest decrease with increasing x.

The low-field magnetic susceptibility $M(H,T)/H$ vs temperature for selected $Sr_{1-x}Ca_xRuO_3$ samples is shown in Fig. 3. The measuring field ($H = 10$ Oe), which was in the ab plane, is sufficiently small enough to represent the zero-field susceptibility, i.e., $(dM/dH)_{H \to 0}$, for all H and T shown. The Curie temperature T_C is unambiguously determined with a low-field-limit ''kink-point'' method. Though T_C is mono-

TABLE I. Parameters of fits to a modified Curie-Weiss law for $Sr_{1-x}Ca_xRuO_3$.

x	Θ (K)	χ_0 (10^{-3} emu/mol)	μ_{eff} (μ_B)
0.00	169	0.9	2.8
0.25	82	2.1	2.8
0.53	57	1.3	2.8
0.83	14	2.9	2.4
0.95	−16	1.1	2.2
1.00	−68	0.7	2.2

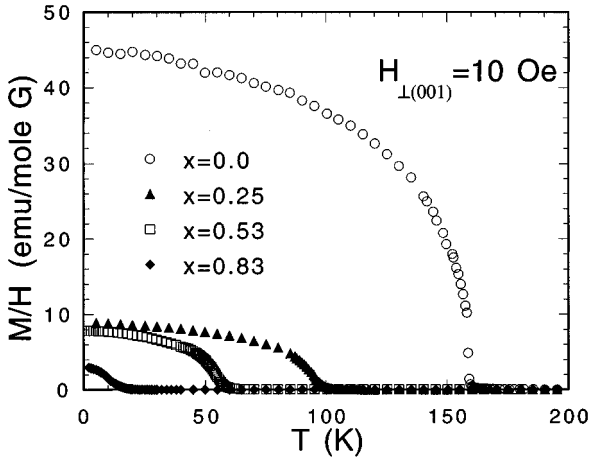

FIG. 3. Low-field magnetic susceptibility ($H=10$ Oe in the ab plane), used to determine the ferromagnetic ordering temperature.

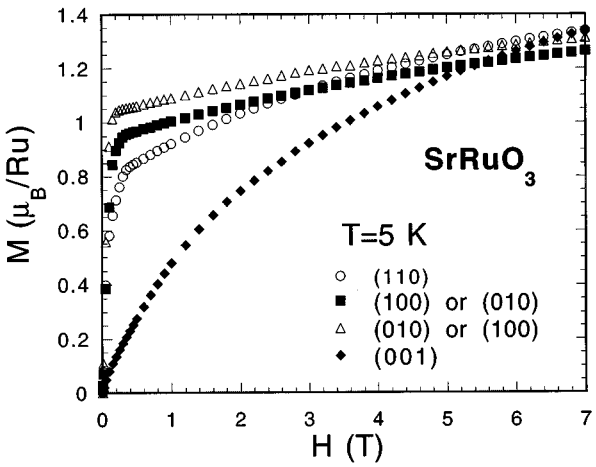

FIG. 5. Magnetic isotherms at $T=5$ K for $x=0$ ($SrRuO_3$) along the principal crystallographic directions.

tonically and smoothly depressed to 0 K for $x=1.0$ ($CaRuO_3$), the depression in the extrapolated $T\rightarrow 0$ K low-field moment is depressed more rapidly.

Figure 4 shows T_C and Θ, the Curie-Weiss temperature, vs x for all samples measured. As noted above, the magnetic ordering persists to $x=1.0$ and the depression of T_C is smooth and monotonic. For $x<0.8$, Θ tracks T_C rather well—as expected for ferromagnetic systems—but a strong deviation between the two occurs for $x>0.8$. This suggests that for large x antiferromagnetic correlations and/or spin fluctuations begin to dominate over long-range ferromagnetic ordering. The magnetic ordering for $x\rightarrow 1.0$ does not have the characteristics of long-range ferromagnetism, but appears to take the form of a short-range, possible spin-glass-like transition. This region is illustrated in the inset of Fig. 4. We present data below on a $x=0.95$ and a $x=0.96$ sample. Returning to an earlier point, even very small, ≈ 1 at. % Sr doping in paramagnetic $CaRuO_3$ is enough to induce magnetic correlations between cation moments.

In Fig. 5 are shown several magnetic isotherms at $T=5.0$ K for a fairly large (2 mg), nearly cubically shaped, single crystal of ferromagnetic $SrRuO_3$ for H along the principle crystallographic directions. As the sample was nearly cubic, demagnetizing corrections should be essentially independent of field direction, and so no corrections were made. It is clear from Fig. 5 that the [100] or [010] direction is the easy axis, rather than [110] asserted in prior work.[17] In a magnetization study of epitaxially grown single-crystal thin films, Klein *et al.*[7] demonstrate that the easy axis is in the ab plane, but with the direction of the easy axis dependent on the temperature, varying by 15° between near T_C and 0 K. The data of Fig. 5 rather dramatically illustrate the anisotropy of magnetization in plane vs out of plane. There is no magnetic hysteresis measurable in $SrRuO_3$ on the scale of this figure.

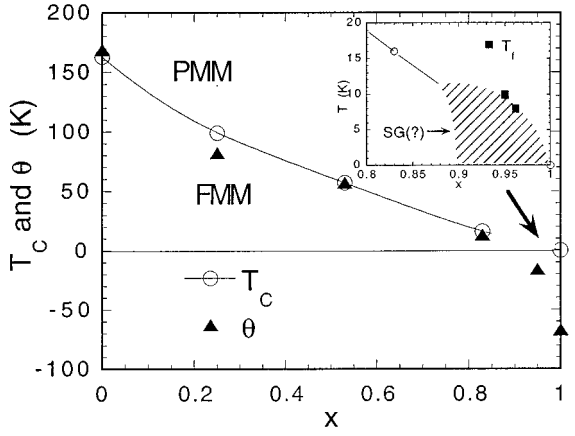

FIG. 4. Magnetic ordering temperature T_C and Curie-Weiss temperature Θ vs x. The inset shows an expanded view of the presumed spin-glass-ordering regime.

In spite of a smooth and uniform decrease in T_C (see Fig. 4), the initial rate of depression of the extrapolated ($T\rightarrow 0$ K) magnetic susceptibility (see Fig. 3) is much more rapid than the rate of depression of T_C. This is due to an increased negative curvature in the low-temperature isothermal magnetization for $x>0$ [see Figs. 6(a) and 6(b)]. The data in Fig. 6 are for $T=5$ K and with H directed along the principal axes, a [100], b [010], and c [001] and along the [110] direction. The data for $H\|[110]$ are not shown in order to reduce clutter in the figure. In all cases, the sample was zero-field cooled (ZFC) through T_C prior to the measurement. Demagnetization effects are not included. Several features of the data of Fig. 6 are notable: First, the initial slope of $M(H)$, $(dM/dH)_{H\rightarrow 0}$, for the mixed samples ($x>0$) decreases rapidly with x, reflecting the rapid decreasing $M/H(T\rightarrow 0\ \mathrm{K})$ seen in Fig. 3. Second, the highest-field magnetization M ($H=7$ T, $T=5$ K) decreases with increasing x. Third, the approach to saturation for the $x=0.25$ sample [Fig. 6(a)] is more rapid for $H\|[001]$ than for the in-plane field (see Fig. 5 for contrast). This suggests that the easy axis tips out of the ab plane and nearer the c axis for this concentration range. For the $x=0.53$ sample, the effect is less strong; i.e., the magnetization does not rise as rapidly for $H\|[001]$. Fourth, for the mixed samples, $M(H,T)$ has a weak steplike structure at low magnetic fields. The steplike structure appears to represent a field-induced spin reorientation, perhaps from out of plane to in plane—a domain rotation on the approach to magnetic saturation. The rapid decrease in M ($H,T>0$ K) for increasing x parallels a strong

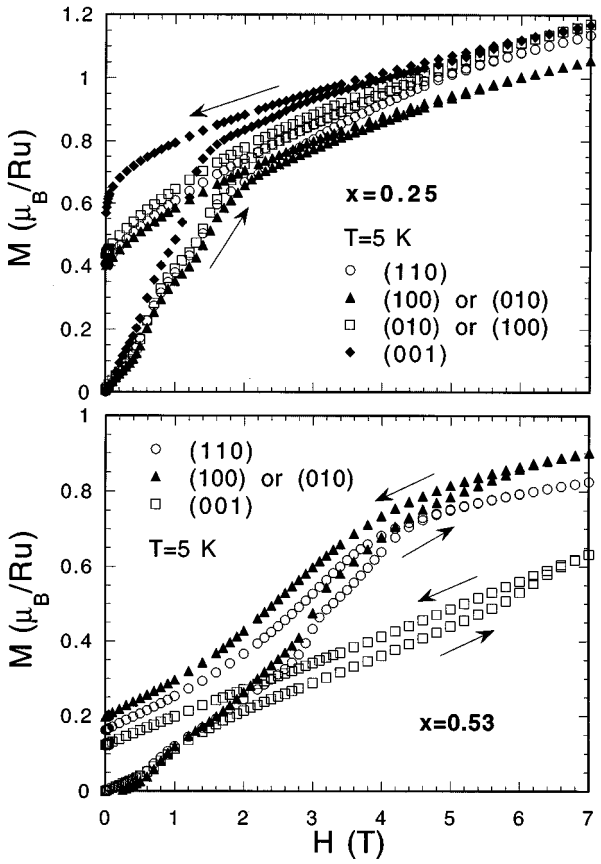

FIG. 6. Magnetic isotherms for two mixed ($x>0$) crystals along principal crystallographic directions. Data for $H\|[110]$ are omitted for clarity. The data for $H\|[001]$ appear to be an easier axis than [100] for the $x=0.25$ sample, in contrast to the data of Fig. 5.

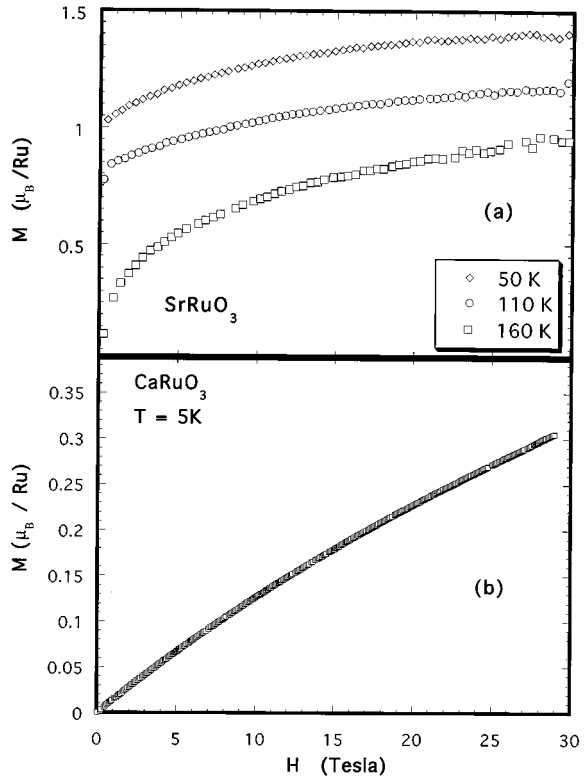

FIG. 7. Magnetic isotherms to very large magnetic fields for ferromagnetic $SrRuO_3$ and paramagnetic $CaRuO_3$. The magnetization for $SrRuO_3$ never reaches the theoretical limit of $2\mu_B$/Ru at highest fields.

increase in hysteresis. (Microscopic studies, such as neutron scattering, may reveal spin orientation in the ordered state for $x>0$ materials and might determine if the moment resides partially on neighboring oxygen for the mixed crystals.[5]) Finally, though there is essentially no discernible hysteresis (very small remanent moment) for the $x=0$ sample, there is a very rapid increase in the remanent moment for $x>0$. [Earlier results on a single-crystal sample reported a significant hysteresis for $SrRuO_3$ (Refs. 16 and 17).] Thus the easy axis for *mixed* single crystals ($x>0$) is not readily determined; e.g., it is less clear that the [110] is *not* the easy axis.[16] Magnetic hysteresis is not an intrinsic physical property, but the large difference in remanence between mixed ($x>0$) and unmixed ($x=0$) ferromagnets, prepared in exactly the same way, is compelling

In Fig. 7(a) we show several magnetic isotherms for $SrRuO_3$ in fields to 30 T, more than twice the field applied in any previous study. To improve signal to noise, several single crystals were stacked with the field parallel to various ab-plane orientations, and so comparison with the lower-field, single-sample data is not precise. The magnetization does not reach the theoretical $S=1$ limit ($2\mu_B$/Ru) even at 30 T, reflecting the itinerant character of the ferromagnetism of $SrRuO_3$. The highest-field slope of the data in Fig. 7, taken to be the Pauli paramagnetism ($\approx 0.002\mu_B$/Ru T), translates to a density of states at the Fermi surface around 500 states/Ry f.u. This should be compared to 166 states/eV atom derived from our heat capacity measurements for $SrRuO_3$ (see below) and to 366 states/Ry f.u. derived from the high-temperature ($T>T_C$) magnetic susceptibility term χ_0. The larger values derived from the high-field slope of M (30 T, 5 K) and from χ_0 may reflect the lack of magnetic saturation on the one hand and the high-temperature ($T>T_C$) χ_0 vs low-temperature ($T\ll T_C$) heat capacity measurements on the other.[18]

In Fig. 7(b) we show magnetization at $T=5$ K to 30 T for paramagnetic $CaRuO_3$. The interesting feature is the curvature to high H seen for $CaRuO_3$. This is reminiscent of $M(H)$ for highly enhanced nonordering paramagnetic metals like Pd or $Pd_{0.95}Rh_{0.05}$,[19] where the curvature is attributed to topological features of the density of states near the Fermi surface in these strongly Stoner enhanced materials. The data may be fit to a Stoner-Edwards-Wohlfarth cubic term, $M=a_1+a_2H+a_3H^3$, with the parameters $a_1=39$ emu/mol, $a_2=6.5\times10^{-3}$ emu/mol Oe, and $a_3=1.2\times10^{-14}$ emu/mol Oe^3. The a_2 coefficient is near to the $T=5$ K value of χ for $CaRuO_3$, the temperature dependence of χ varying strongly in that temperature region.

A rather remarkable feature of the $Sr_{1-x}Ca_xRuO_3$ system is that the magnetic ordering temperature appears to decrease to 0 K only for $x=1.0$ (see Fig. 4). This means the present data do not permit an identification of a critical concentration Sr required to produce magnetic order. This result has focused our attention on dilute Sr doping in $CaRuO_3$. We performed several very-low-field magnetization studies on two single-crystal $Sr_{0.05}Ca_{0.95}RuO_3$ samples $x=0.95$ and x

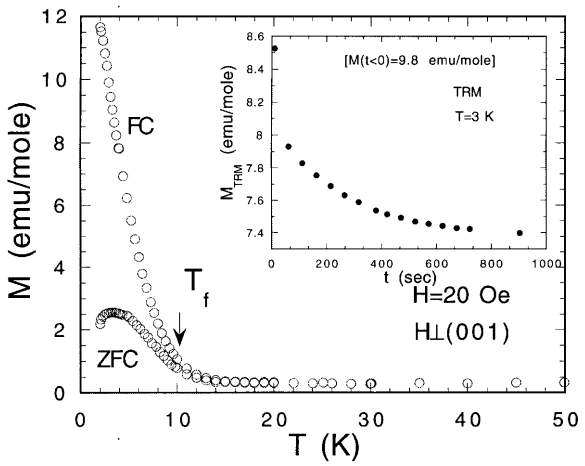

FIG. 8. Low-field magnetization and thermoremanent magnetization for the $x=0.95$ sample showing spin-glass-like behavior.

$=0.96$. (The uncertainty in the measured x, which is found from EDX-SEM measurements, is about ± 0.005.)

Figure 8 shows the low-field (20-Oe) magnetization on this sample, both zero-field cooled (ZFC) and field cooled (FC). The difference in the ZFC and FC data is typical of spin glass or short-range ordering and unlike comparable data on this system for $x<0.83$ samples. We also performed low-field time-dependent thermoremanent magnetization measurements. The data were obtained in the following manner: The sample was warmed to 30 K, well above what appears to be the low-field magnetic irreversibility temperature $T_f \approx 10$ K, the divergent point in the ZFC and FC 20-Oe $\chi(T)$ data. A field of 20 Oe was applied, the sample cooled to $T \leqslant T_f$, a waiting time established (5000 s), and then the field reduced to zero, whereupon the magnetization measured as a function of time, for about 1 h. As is characteristic of a possible spin glass, M $(H \rightarrow 0,\ t>0)$ decreased quickly to a nonzero value, followed by a very slow relaxation of M over time. For $T \geqslant T_f$, the relaxation to $M=0$ is rapid. Representative data for $T=3.0$ K are shown in the inset of Fig. 8.

To our knowledge, this is the first indication of spin-glass-type behavior in a $4d$ transition-metal oxide. This suggests that Ru moments are correlated when only a small number of Sr ions are randomly located in the lattice, further suggesting that the magnetic order may be characteristic more of a spin glass or other short-range order than of long-range ferromagnetism. Additional measurements are under way in order to better characterize this interesting regime of the $Sr_{1-x}Ca_xRuO_3$ system ($x \geqslant 0.83$) and to assess various fits to magnetic relaxation models, including the stretched exponential $M(t)=M_0 \exp[-(at)^{\alpha}]$.

EXPERIMENTAL RESULTS: HEAT CAPACITY

In Fig. 9 we show results of specific heat, $C(T)$, measurements for several $Sr_{1-x}Ca_xRuO_3$ samples taken in zero applied field for $2<T<20$ K. A representative plot of $C(T)/T$ vs T^2 is shown in the inset of Fig. 9(a) along with the linear fit to the data. In all cases, the electronic specific heat coefficients γ are rather large. The value of γ

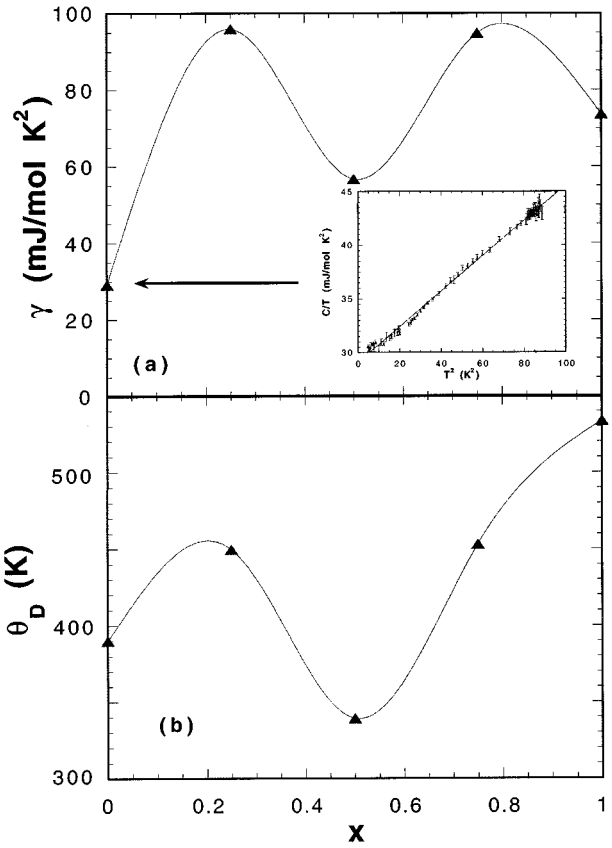

FIG. 9. Parameters of fits to the low-temperature specific heat, $C/T=\gamma+\beta(\Theta_D)T^2$ vs T^2 as a function of x. The inset shows $C(T)$ vs T^2 for $SrRuO_3$.

(29 mJ/mol K^2) for our 3-mg $x=0$ single-crystal sample agrees very well with the 47-mg polycrystalline sample result of Allen *et al.*[4] (30 mJ/mol K^2). Comparing our measured γ to the density-of-states calculations of Allen *et al.*[4] (190 states/Ry cell for both spin up and spin down) yields a mass enhancement $m^*=3.4m_0$. Comparison with the density-of-states calculations by Singh[19] for the orthorhombic $SrRuO_3$ structure (225 states/Ry cell) yields $m^*=3.0m_0$. Both band structure calculations[4,19] apply to the orthorhombic $SrRuO_3$ ferromagnetic phase.

From electron-energy-loss spectroscopy measurements of the plasma frequency,[20] where $\omega_p \approx (m^*)^{(-1/2)}$, one obtains a somewhat larger ($\approx 7.0m_0$) effective mass for $SrRuO_3$. It is not surprising that quasiparticle masses differ, depending on the measurement made and which comparison to theory is used, but the effective mass derived from a measurement of the plasmon frequency[20] should be closer to the calculated single-particle mass and that derived from heat capacity measurements, not further from the unrenormalized mass.[21] Also, Ref. 20 suggests an increase in the density of states at the Fermi surface, progressing from $CaRuO_3$ to $SrRuO_3$ to $BaRuO_3$, which is not found in our low-temperature heat capacity data.

Large heat capacity coefficients are characteristic of most of the members of the Ruddlesdon-Popper[22] series $(Sr_{1-x}Ca_x)_{n+1}Ru_nO_{3n+1}$, $n=1-\infty$. Allen *et al.*[4] point out that the enhancement of γ is due more to spin fluctuations than to phonon mass enhancement. This is consistent with

our observations that in $CaRuO_3$, which though not magnetically ordered has a large electronic heat capacity, $\gamma = 73$ mJ/mol K^2, and it is a borderline magnetic material based on our Ru sublattice chemical substitution studies,[13–15] as well as small Sr doping on the Ca sublattice (see above). Unfortunately, to our knowledge, no band structure calculations exist for $CaRuO_3$. It is tempting to assume, however, that the density of states is at least comparable to $SrRuO_3$, in which case the mass enhancement from specific heat would be around $(5-6)m_0$. This is at least consistent with plasma frequency results of Ref. 20, showing $m^* \approx 8.0$, slightly larger for $CaRuO_3$ compared to $SrRuO_3$.[20]

The unusual nonmonotonic dependence on x of γ [Fig. 9(a)] and of the Debye temperature Θ_D [Fig. 9(b)] is surprising, given the smooth monotonic decrease in T_C (Fig. 4) and the saturation magnetic moment [M ($H=7$ T, $T=5$ K) from Figs. 5 and 6]. The decrease in γ seen in Fig. 9(a) for $x = 0.5$ is reproducible, the figure showing results for two samples of almost identical composition from entirely different batches. The calculation of Θ_D for those two samples is essentially identical, and so only one data point is shown in Fig. 9(b).

Finally, we attempted a search for spin-wave contributions to the heat capacity by trying to include in the temperature dependence of the low-temperature heat capacity a $T^{(3/2)}$ term for $SrRuO_3$ and other ferromagnetic samples. However, none of the data showed a satisfactory fit with this term included.

EXPERIMENTAL RESULTS: TRANSPORT PROPERTIES

In Fig. 10 we show the in-plane electrical resistivity as a function of temperature, $\rho(T)$, for the $x=0$, 0.53, and 1.0 $Sr_{1-x}Ca_xRuO_3$ samples. The out-of-plane resistivity (current along the c axis) has a similar temperature dependence, but is slightly larger ($\approx 10\%$) in magnitude, reflecting a small anisotropy expected because of the orthorhombic symmetry. Uncertainty in the area/length measurements precludes knowing the absolute value of resistivity to better than about 10%. In single-crystal metallic Sr_2RuO_4, which is the $n=1$ Ruddlesdon-Popper structure and which has a single layer, i.e., a much more anisotropic structure than $Sr_{1-x}Ca_xRuO_3$, the c-axis resistivity $\rho_c(T)$ is semiconductorlike for $50 < T < 300$ K, and ρ_c/ρ_{ab} reaches as high as ≈ 500.[23]

The temperature dependence of $\rho(T)$ for $SrRuO_3$ is similar to reports for thin films by Allen *et al.*[4] and Klein *et al.*[7] including the break at T_C. However, with $\rho = 4\ \mu\Omega$ cm at low T for our samples, the single crystals are more highly conductive at low temperature. The room-temperature resistivity is also similar to another single-crystal data report.[16] Though $\rho(T)$ for $SrRuO_3$ tends to ''bottom'' out like any metal with impurity-limited resistivity, $CaRuO_3$ continues to decrease and becomes even lower for $T<5$ K. [We are continuing to track $\rho(T)$ for this material down to much lower temperatures.]

The data of Fig. 10(a) are indicative of the high quality of the single-crystal samples: $R_{300}/R_5 \approx 51$ for $SrRuO_3$ and ≈ 43 for $CaRuO_3$. As in the thin-film material, we estimate a room-temperature quasiparticle transport mean free path $l \approx 10$ Å, demonstrating $k_F l \approx O(1)$. This would suggest that

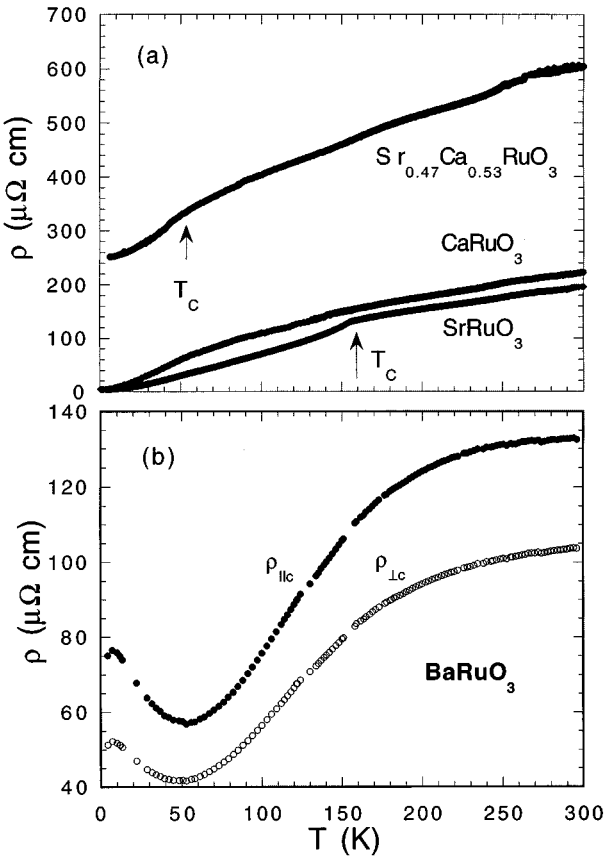

FIG. 10. Electrical resistivity vs temperature for $x=0$, $x=0.47$, and $x=1.0$ samples and anisotropy of electrical resistivity for a companion material $BaRuO_3$.

$SrRuO_3$ and orthorhombic $CaRuO_3$, assuming similar band structure character in this paramagnetic regime, are ''bad'' metals.[24] That both $SrRuO_3$ and $CaRuO_3$ are close to being nonmetals ($d\rho/dT<0$ as $T\rightarrow 0$ K) is demonstrated by in-plane and out-of-plane doping studies from our group.[13,14] Focusing on the high-temperature resistivity, we see the mixed crystal ($x=0.47$) has ρ at room temperature nearly 3 times the others. This would be expected from Nordheim's rule, though the meaning of such a classical notion in the case of ''bad'' metals is not clear.[24] The room-temperature mean free path for this sample may be only 2–3 Å.

While not a principal subject of this paper, we show in Fig. 10(b) similar data for single-crystal $BaRuO_3$, which has a somewhat different crystal structure—a staggered c-axis stacking of RuO chains with face-sharing and corner-sharing Ru-O octahedra. The unit cell is approximately twice as large as that for $SrRuO_3$ and $CaRuO_3$. This probably comes about because the Ba ionic radius (1.36 Å) is larger than that for the ideal perovskite. The $\rho(T)$ of $BaRuO_3$ is uniformly larger than that for $SrRuO_3$ or $CaRuO_3$, and the R_{300}/R_5 is considerably less than for the others. Also shown is $\rho_c(T)$, with current directed along the c axis. Though the temperature dependence is essentially the same, the magnitude is 1.3 as large, reflecting the higher anisotropy in this system. (Comparable data for $SrRuO_3$ and $CaRuO_3$ show less anisotropy, $\rho_c/\rho_a \approx 1.1$.) It is notable that the high-temperature dependence of ρ in $BaRuO_3$ is different from that for

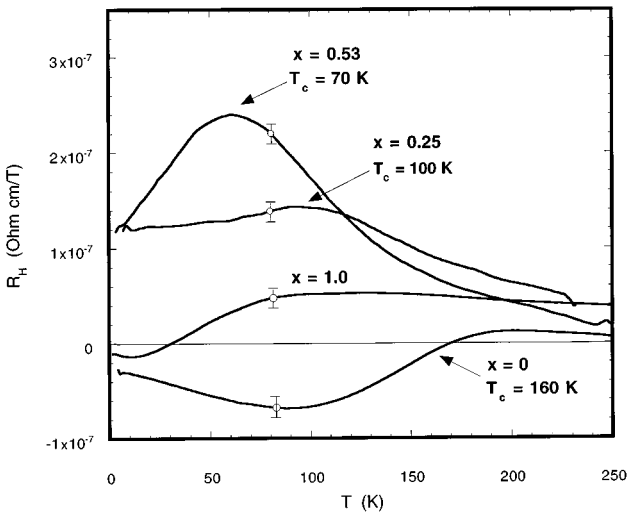

FIG. 11. Hall constant vs temperature for four samples. Note the sign reversal for the $x=0$ and $x=1.0$ samples, but not the others. Data were taken in $H=10$ T magnetic fields. Error bars are representative of the full temperature range.

$SrRuO_3$ or $CaRuO_3$, where ρ increases linearly with temperature, characteristic of bad metals. Another anomaly is the nonmonotonic behavior of $\rho(T)$ for $T<50$ K for $BaRuO_3$. This is highly reproducible from sample to sample, and at present we have no explanation for this behavior. We are currently tracking this resistivity to $T\ll 2$ K.

None of the data of Fig. 10 show conventional metallic behavior; e.g., fits to the Bloch-Gruneisen formulas are not successful. Furthermore, Klein *et al.*[7] have pointed out that even though $\rho(T)$ displays classic Fisher-Langer behavior for $T<T_C$, $d\rho(T)/dT$, and $C(T)$, dT for $SrRuO_3$ show unusually strong divergence at T_C and with large critical exponents. This is attributed to the bad metal characteristics of the material.

In Fig. 11 we show Hall effect data taken at $H=10$ T for four $Sr_{1-x}Ca_xRuO_3$ samples. As in Ref. 9, there is a sign reversal from electronlike (negative R) to positive with increasing temperature for the $x=0$ and $x=1.0$ samples, at $T\cong 170$ K for $SrRuO_3$ and $T\cong 30$ K for $CaRuO_3$. Gausepohl *et al.*[9] have performed their measurements on thin-film samples, and our data agree reasonably well with those data: The sign reversal for the thin-film samples is at about 150 K for $SrRuO_3$ and 55 K for $CaRuO_3$. In addition, the extraordinary Hall effect in $SrRuO_3$ is evident in both cases; the Hall voltage vs field is linear for paramagnetic $CaRuO_3$ for all temperatures, but is highly nonlinear for ferromagnetic $SrRuO_3$ below the Curie temperature. Though the sign reversal indicates multiband contributions to the Hall conductivity, we can estimate from our data the density of carriers in the extreme temperature limits: For $SrRuO_3$, $n_e \approx 3\times 10^{22}$ cm^{-3} at $T=5$ K and $n_p \approx 6\times 10^{22}$ cm^{-3} holes at $T=200$ K; for $CaRuO_3$, $n_e \approx 3\times 10^{22}$ cm^{-3} and $n_e \approx 1\times 10^{22}$ cm^{-3} at 200 K. While these do not agree particularly well quantitatively with the thin-film results, the agreement in temperature dependence is reasonable. The low density of carriers and sign reversal hint at the complexity of the band structure for these materials and suggests that they may be compensated metals.

In view of the general agreement on Hall voltage sign reversal in the end members of the $Sr_{1-x}Ca_xRuO_3$ system, it is surprising that there is no sign reversal for the samples in the mixed regime. Data are shown in Fig. 11 for the $x=0.50$ and $x=0.25$ samples. The density of carriers, again using a single-band model, would be around 3×10^{21} cm^{-3} at $T=5$ K for both mixed crystals. This is at least consistent with the higher longitudinal resistivity for the mixed crystals. The origin of the sign reversal for the end member samples remains open to speculation. Because it occurs for paramagnetic $CaRuO_3$, it is not intrinsically related to the itinerant magnetization of $SrRuO_3$, but is probably related to scattering from different parts of the Fermi surface, hole pockets, and electron regions. That the sign reversal occurs for both lends support to the notion that the Fermi surfaces are similar for the two materials. That this sign reversal does not occur for the mixed crystals may be related to the additional scattering introduced by disorder on the Sr, Ca anion sublattice, thus preventing a temperature-driven saturation of low-temperature (electron-dominated) scattering.[9]

CONCLUSIONS

The $Sr_{1-x}Ca_xRuO_3$ pseudoternary system is rich in physical effects attributable to the highly correlated Ru $4d$-electron bands. Though all the data presented show metallic behavior, they are easily switched from the metallic to nonmetallic state through chemical substitution. This is consistent with recent data on other Ru $4d$ transition-metal oxides which are also borderline insulators.[25] The advantage of single-crystal data is evident from this study. For example, the large magnetocrystalline anisotropy has been demonstrated for $x>0$ materials. This may be reflected in the Hall effect data, which show sign reversal as a function of temperature for the end member systems, $x=0$ and $x=1.0$, but not for the mixed systems. The very-high-field magnetization, which does not saturate even for 30 T at low temperatures, lends support for the itineracy of the materials. Further work will involve microscopic studies (neutron scattering) to determine the spin orientation in $Sr_{1-x}Ca_xRuO_3$ as a function of x as well as infrared and angle-resolved photoemission spectroscopy measurements to assist in understanding the electronic band properties of these ''bad'' metals.[25] The possible spin-glass-type magnetism for samples with only a small amount Sr doping in paramagnetic $CaRuO_3$ deserves more extensive investigations. Finally, all the results bear on the interesting subject of transport, magnetic itineracy, and thermodynamic properties of ''bad'' metals.

ACKNOWLEDGMENTS

The authors would like to express thanks to Michael Davidson and Robert Goddard for assistance in sample characterization and Steven Hill and Vladimir Dobrasavljevic for useful discussions. Support of the NHMFL is by the National Science Foundation under Cooperative Agreement No. DMR95-27035 and the State of Florida.

*On leave at National High Magnetic Field Laboratory, Florida State University, Tallahassee, Florida 32310.
[1] J. J. Randall and R. Ward, J. Am. Chem. Soc. **81**, 2629 (1959).
[2] J. B. Goodenough, Czech. J. Phys. B **17**, 304 (1967).
[3] See P. A. Cox, *Transition Metal Oxides* (Clarendon, Oxford, 1995).
[4] P. B. Allen, H. Berger, O. Chauvet, L. Forro, T. Jarlborg, A. Junod, B. Revaz, and G. Santi, Phys. Rev. B **53**, 4393 (1996).
[5] S. Nagler (private communication).
[6] Y. Maeno, H. Hashimoto, K. Yoshida, S. Ishizaki, T. Fujita, J. G. Bednorz, and F. Lichtenberg, Nature (London) **372**, 532 (1994).
[7] L. Klein, J. S. Dodge, C. H. Ahn, G. J. Snyder, T. H. Geballe, M. R. Beasley, and A. Kapitulnik, Phys. Rev. Lett. **77**, 2774 (1996).
[8] J. J. Neumeier, A. L. Cornelius, and J. S. Schilling, Physica B **198**, 324 (1994); M. Shikano, T.-K. Huang, Y. Inaguma, M. Itoh, and T. Nakamura, Solid State Commun. **90**, 115 (1994).
[9] S. C. Gausepohl, M. Lee, R. A. Rao, and C. B. Eom, Phys. Rev. B **54**, 8996 (1996).
[10] T. Kiyama, K. Yoshimura, K. Kosuge, Y. Ikeda, and Y. Bando, Phys. Rev. B **54**, R756 (1996).
[11] G. L. Catchen, T. M. Rearick, and D. G. Schlom, Phys. Rev. B **49**, 318 (1994).
[12] T. C. Gibb, R. Greatrex, N. N. Greenwood, and P. Kaspi, J. Chem. Soc. Dalton Trans. **1973**, 1253 (1973). Our own data show no evidence for ordering above $T = 1$ K.
[13] M. Shepard, G. Cao, S. McCall, F. Freibert, and J. E. Crow, J. Appl. Phys. **79**, 4821 (1996).
[14] G. Cao, S. McCall, J. Bolivar, M. Shepard, F. Freibert, P. Henning, T. Yuen, and J. E. Crow, Phys. Rev. B **54**, 15 144 (1996).
[15] G. Cao, F. Freibert, and J. E. Crow, J. Appl. Phys. **81,** 3885 (1997).
[16] C. B. Eom, R. J. Cava, R. M. Fleming, J. M. Phillips, R. B. van Dover, J. H. Marshall, J. W. P. Hsu, J. J. Krajewski, and W. F. Peck, Jr., Science **258**, 1766 (1992).
[17] A. Kanbayasi, J. Phys. Soc. Jpn. **41**, 1876 (1976).
[18] A. Kanbayasi, J. Phys. Soc. Jpn. **44**, 89 (1978).
[19] S. Foner and E. J. McNiff, Jr., Phys. Lett. **29A**, 28 (1969); M. T. Beal-Monod, Physica B & C **109&110B**, 1837 (1982); J. J. M. Franse, J. Magn. Magn. Mater. **31**, 812 (1983); D. Singh (unpublished).
[20] P. A. Cox, R. G. Egdell, J. B. Goodenough, A. Hammett, and C. C. Naish, J. Phys. C **16**, 6221 (1983); See A. Gulino, R. G. Egdell, P. D. Battle, and S. H. Kim, Phys. Rev. B **51**, 6827 (1995), for data on related systems.
[21] J. Caulfield, W. Lubczynski, F. L. Pratt, J. Singleton, D. Y. K. Ko, W. Hayes, M. Kurmoo, and P. Day, J. Phys. Condens. Matter. **6**, 2911 (1994); S. Hill (private communication).
[22] S. N. Ruddelsdon and P. Popper, Acta Crystallogr. **10**, 538 (1957).
[23] Y. Maeno, H. Hashimoto, K. Yoshida, S. Nishizaki, T. Fujita, J. G. Bednorz, and P. Lichtenberg, Nature (London) **372**, 532 (1994).
[24] V. J. Emery and S. A. Kivelson, Phys. Rev. Lett. **74**, 3253 (1995).
[25] G. Cao, S. McCall, J. E. Crow, and R. P. Guertin, Phys. Rev. Lett. **78**, 1751 (1997).